Fatigue Analysis of Hip Prosthesis

Prof. Dr.Adnan N. Jameel Dr.Wedad I. Majeed Alaa Mohammed Razzaq

Dep.of Mech.
College of Engineering
University of Baghdad

Abstract

The present work covers the analytical design process of three dimensional (3-D) hip joint prosthesis with numerical fatigue stress analysis. The analytical generation equations describing the different stem constructive parts (ball, neck, tour, cone, lower ball) have been presented to reform the stem model in a mathematical feature. The generated surface has been introduced to FE solver (Ansys version 11) in order to simulate the induced dynamic stresses and investigate the effect of every design parameter (ball radius, angle of neck, radius of neck, neck ratio, main tour radius, and outer tour radius) on the max. equivalent stresses for hip prosthesis made from titanium alloy. The dynamic loading case has been studied to a stumbling case. The load has been applied on the cap tip as a concentrated load distributed on the interface of ball and socket. The results show that the decreasing of max. Fatigue stress by (175) MPa could be obtained by increasing the outer tour radius from (10)mm to (15) mm and that will change the max. Fatigue zone location from the tour section to the neck. The ball radius and neck angle must be as lower as possible to decrease the fatigue stresses. The most dominate parameter to increase the safety factor is the radius of neck.

Key words: Stem modeling, Hip implant, Hip prosthesis, Fatigue analysis.

الخلاصة:

هذا العمل يغطي تصميم بديل مفصل الورك ثلاثي الابعاد مع التحليل العددي لاجهادات الكلال. معادلات التوليد النظرية التي تصف الاجزاء البنائية للبديل (الكرة، العنق، الوصلة، المخروط، الكرة السفلى) تم تقديمها لتكوين نموذج البديل بصورة رياضية . اما ادخال السطح المولد الى محلل العناصر المحددة (Ansys version 11) لمحاكاة الاجهادات الديناميكية المتولدة ودراسة تأثير كل متغير (نصف قطر الكرة العليا، زاوية ميل العنق، نصف قطر العنق، نسبة العنق، نصف قطر الوصلة الرئيسي، نصف قطر الوصلة الخارجي) على الاجهادات العظمى المكافئة لبديل ورك مصنوع من سبيكة التيتانيوم حالة التحميل الديناميكية درست لحالة التعثر . تم تسليط حمل مركز على قمة غطاء المفصل وموزعاً على سطح الكرة والتجويف. اظهرت النتائج بأنه يمكن تقليل اجهاد الكلال الاعظم بمقدار 175 ميكا باسكال بزيادة نصف قطر الوصلة الخارجي من (10) الى (15) ملم و ذلك سوف يغير موقع منطقة اعظم اجهاد كلال من مقطع الوصلة الى منطقة العنق. نصف قطر الكرة و زاوية العنق يجب ان يكونا باقل مايمكن لتقليل اجهادات الكلال. المتغير الاكثر تاثيرا في زيادة معامل الامان هو نصف قطر العنق.

1.1. Introduction

Model generation means a process of generating the nodes and elements that represent the spatial volume and connectivity of the actual system [Kassim, 1997]. The accurate geometrical representation of stem surface is the first step to a successful computerized stem design which represents base of subsequent analysis such as static stress analysis (combined and contact), fatigue stress investigation, impact stress and vibration to ensure a successful stem implant design. This paper presents a mathematical model able to compute the different surfaces of stem joint (upper ball, neck, tour, cone, and lower ball). The numerical representation of the prosthesis surface how to choice the element type, how to apply load and an overview to fatigue theory are presented at last, The adopted stress analysis fatigue theory is soderberg theory with a high cyclic loading.

1.2. Literature Survey

T. P. Colleton et al (1993) [13] described the cement mantle of an artificial hip joint and subjected to detailed failure analysis. Results from a finite element analysis were used, together with the techniques of fracture mechanics, in an attempt to explain the magnitude and direction of fatigue cracking. Fracture mechanics calculations indicate that the local stress intensity in the region of the principal defect would have been sufficient to exceed the threshold for fatigue crack propagation in this material.

B.A.O. McCormack and P. J. Prendergas(1999) [14] show how fatigue damage accumulation occurs in the cement layer of a hip replacement, a physical model of the joint was used in an experimental study. The model generates the stress pattern found in the cement layers whilst at the same time allowing visualization of micro crack initiation and growth. In this way the gradual process of damage accumulation can be determined. Six specimens were tested to 5 million cycles and a total of 1373 cracks were observed. It was found that, under the flexural loading allowed by the model, the majority of cracks come from pores in the bulk cement. Furthermore, the lateral and medial sides have statistically different damage accumulation behaviors, and pre-load cracks significantly accelerate the damage accumulation process. The experimental results confirm that damage accumulation is continuously increasing with load in the form of crack initiation and crack propagation.

A. Z. Senalp et al(2007) [9] study dynamic stresses varying in time and resulting in the fatigue failure of implant material. In this study, four stem shapes of varying curvatures for hip prosthesis were modeled. Static, dynamic and fatigue behavior of these designed stem shapes were analyzed using commercial finite element analysis ANSYS software. Static analyses were conducted under body load. Dynamic analyses were performed under walking load. Fatigue behavior of stem shapes was predicted using ANSYS Workbench software. Performance of the stem shapes was investigated for Ti–6Al–4V and cobalt–chromium metal materials and compared with that of a commonly used stem shape developed by Charnley.

T. P. Andriacchi et al(2009) [22] used two-dimensional stress analysis to study the effects of some of the factors leading to early fatigue failure of the femoral stem in total hip prosthesis.

The results show that loss of proximal stem support at the level of the calcar femorale will result in stem stress levels which can lead to fatigue failure, in addition, the role of the body weight and range of cyclic stress fluctuation play an important role in fatigue life under conditions where the stem has lost proximal support.

These results indicate that stem design could be improved by incorporating some means of ensuring adequate support at the calcar femoral and by increasing cross sections in the middle one-third of the stem where maximum tensile stresses are found to occur.

2. Mathematical Representation

Herein three dimensional (3-D) model representation of a hip joint prosthesis consists of five constructive parts will be derived analytically depending on each part shape. The different stem parts are:

1- Bottom sphere
2- Cone
3- Tour interface
4- Neck
5- Upper sphere

The equations that generate the whole surface are:-

Bottom Sphere: This surface is a half sphere which represents the bottom of stem and its equations are [Fumihiro and ko, 2002]:

$$x^2 + y^2 + z^2 = r^2 \quad (1)$$

The spherical coordinate system relates to the Cartesian system in the following equations [Niel Pieterse, 2006]:

$$\left.\begin{aligned} x &= r_i * \cos\theta * \cos\emptyset \\ y &= r_i * \sin\theta \cos\emptyset \\ z &= r_i * \sin\emptyset \end{aligned}\right\} \quad (2)$$

The different variables in eq.(2), (r_i) is the bottom sphere radius, $\theta = 0$ to 360 degree, $\emptyset = 0$ to 180 degree are shown in Figure (1).

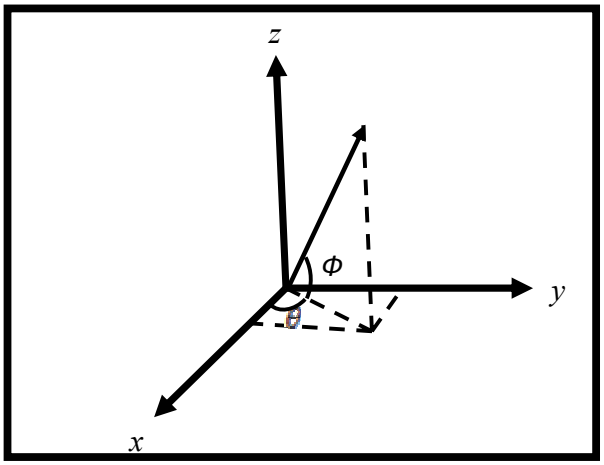

Figure (1), Spherical coordinates System Coordinate

Cone Surface: This section is so important in the fixation of stem in femur and it is non-complete cone. The generation's equations for any cone section are:

$$x^2 + y^2 = r^2 \quad (3)$$

Where (r) is a function of (z) see Figure (2). From the trigonometric relationship the following equations could be concluded:

$$\left.\begin{aligned} r_o/(l + z_1) &= (r_o - r_i)/l \\ z_1 &= (l * r_i)/(r_o - r_i) \end{aligned}\right\} \quad (4\text{- a})$$

Where (r_o) is the upper cone radius, (r_i) is the bottom cone radius and (l) is the cone length then:

$$r = (z + z_1)(r_o - r_i)/l \quad (4\text{- b})$$

Sub eq.(4 - a) in eq.(4 - b) to get:

$$r = z(r_o - r_i)/l + r_i \quad (5)$$

And

$$\left.\begin{aligned} x &= r * \cos\theta \\ y &= r * \sin\theta \end{aligned}\right\} \quad (6)$$

Where (θ) = 0 to 360 degree.

Sub eq.(5) in eq.(6) to get:

$$\left.\begin{aligned} x &= (z(r_o - r_i)/l + r_i)\ Cos\ (\theta) \\ y &= (z(r_o - r_i)/l + r_i)\ \sin\theta \end{aligned}\right\} \quad (7)$$

From eq.(7) it is clear that :

$x = f\ (z, \theta)$ *and* $y = f\ (z, \theta)$ where (θ) = 0 to 360 degree and z = 0 to (l).

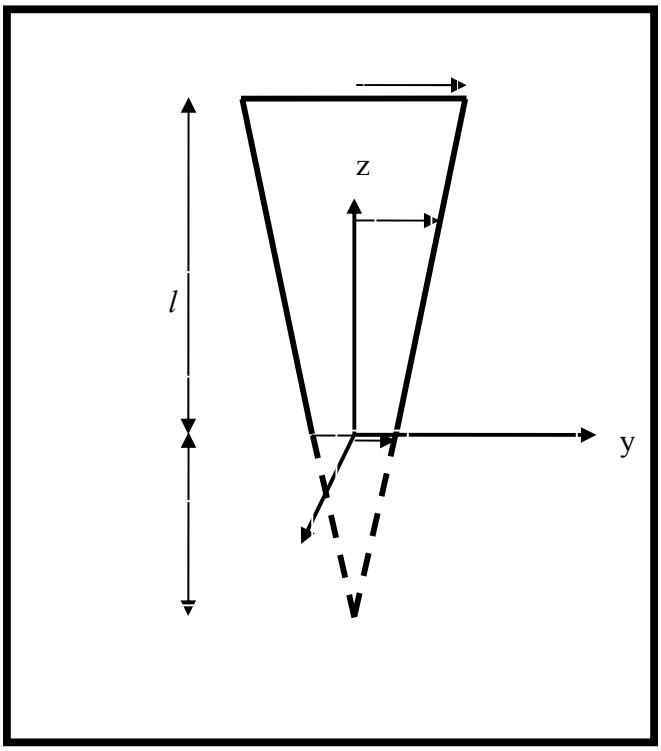

Figure (2), Cone Section

Tour Interface: Figure (3) shows the tour interface surface which represents the third section of stem prosthesis.

$$x^2 + y^2 = r^2$$

If (r) The outer cone radius (r_o) so that :

$$x^2 + y^2 = r_o^2 \qquad (8)$$

Where:

$$x = r_o * \cos\theta$$
$$y = r_o * \sin\theta$$
$$z = l$$

Where (θ) = 0 to 360 degree

The coordinate transformation from circle center (o_c) to tour center (o_t) see Figure (4), are:

$$\left.\begin{aligned} x_t &= x_c \\ y_t &= y_c + r_t \\ z_t &= z_c \end{aligned}\right\} \qquad (9)$$

Where (r_t) is the tour main radius.

From Figure (4), y_t and z_t system inclined from y_t and z_t by (θ_t), x_t and x_{t1} are coincide with each other, that:

$$\left.\begin{aligned} x_{t1} &= x_t \\ y_{t1} &= y_t * cos(\theta_t) + z_t * sin(\theta_t) \\ z_{t1} &= z_t cos(\theta_t) - y_t sin(\theta_t) \end{aligned}\right\} \qquad (10)$$

Where (θ_t) is the tour angle (neck angle).

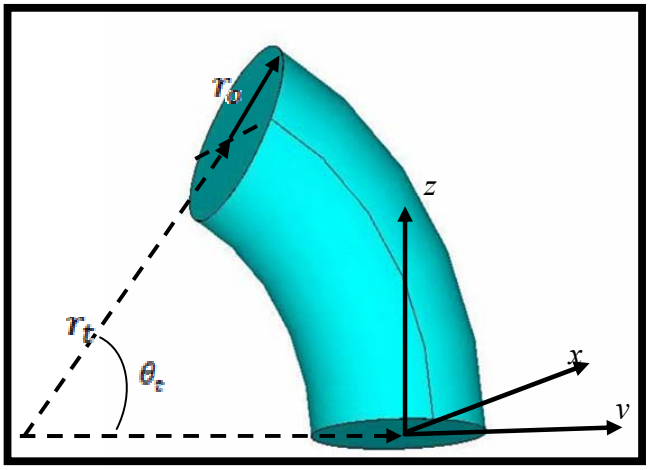

Figure (3), Tour Interface

Neck surface: which represent the weakest part in the system so that it must be studied and analyzed carefully.

This section allows more freedom in the joint movement. Figure (5) shows the neck surface and the different surface variables .In this Figure the coordinate system S_n is fixed at the middle of neck piece and it's clear that (r) is a f (θ_1, θ_2) so that :

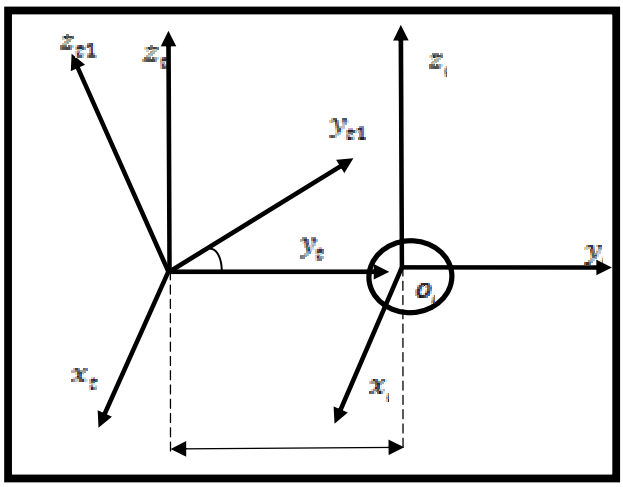

Figure (4), Transformation of Tour Coordinate.

$$\left.\begin{aligned} x_n &= 0 \\ y_n &= r_n + r_{on}\,(1-\cos(\theta_i)) \\ z_n &= r_{on} * \sin(\theta_i) \end{aligned}\right\} \quad (11)$$

Where (i=1 for Bottom part and i=2 for upper part)

The coordinate transformation from S_n to S_{n1} are shown in Figure (6) and as following:

$$\left.\begin{aligned} x_{n1} &= x_n \\ y_{n1} &= y_n \\ z_{n1} &= z_n + r_{on} * \sin(\theta_1) \end{aligned}\right\} \quad (12)$$

The generation of neck surface is achieve by rotating x_{n1}, y_{n1} about z_{n1} are in Figure (7).

$$\left.\begin{aligned} x_{n2} &= x_{n1}\cos(\theta) + y_{n1}\sin(\theta) \\ y_{n2} &= y_{n1}\cos(\theta) - x_{n1}\sin(\theta) \\ z_{n2} &= z_{n1} \end{aligned}\right\} \quad (13)$$

Figure (8) shows the transformation from $S_{n2}$to S_{n3}

$$\left.\begin{aligned} x_{n3} &= x_{n2} \\ y_{n3} &= y_{n2} + r_t \\ z_{n3} &= z_{n2} \end{aligned}\right\} \quad (14)$$

where (r_t) It is the tour main radius.

The last transformation is to be from S_{n3} to S_{n4} coordinate system as in Figure (8).

$$\left.\begin{aligned} x_{n4} &= x_{n3} \\ y_{n4} &= y_{n3}\cos(\theta t) + z_{n3}\sin(\theta t) \\ z_{n4} &= z_{n3}\cos(\theta t) - y_{n3}\sin(\theta t) \end{aligned}\right\} \quad (15)$$

The coordinate transformation from S_{n4} to S_{n5} are :

$$\left.\begin{aligned} x_{n5} &= x_{n4} \\ y_{n5} &= y_{n4} - r_t(1-\cos(\theta t)) \\ z_{n5} &= z_{n4} + l + r_t\sin(\theta t) \end{aligned}\right\} \quad (16)$$

as in Figure (8).

Upper Sphere Surface: The generation of upper sphere is different from the Bottom sphere surface, it is larger than a half sphere in surface and that depend upon the difference between the upper neck side radius and the upper sphere radius see Figure (9). The other difference is coordinate transformation. Where x_b, $y_b$and z_b can be evaluated from Eq. (2).

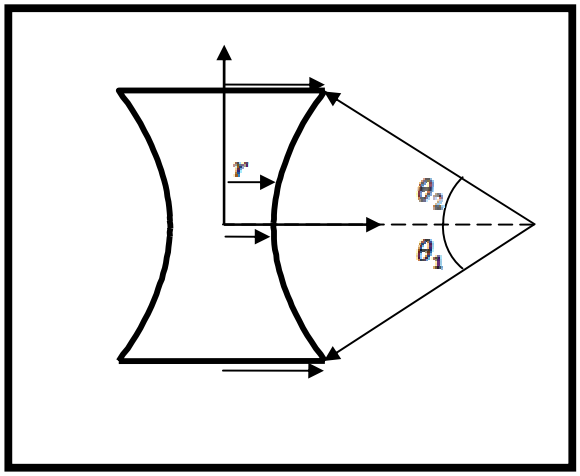

Figure (5), Neck of Stem.

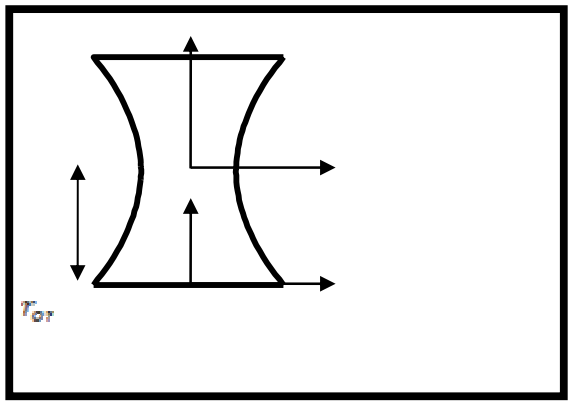

Figure (6) Coordinate Transformation from S_n to S_{n1}.

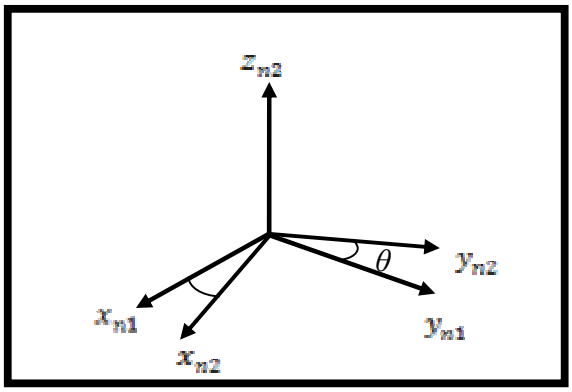

Figure (7) Generation of Neck surface.

In Figure (10) the coordinate transformation from S_b to S_{b1} ,coordinate system as follows:

$$\left.\begin{aligned} x_{b1} &= x_b \\ y_{b1} &= y_b \\ z_{b1} &= z_b + A \\ A &= \sqrt[2]{r_b{}^2 - r_{on}{}^2} \end{aligned}\right\} \quad (17)$$

Where (A) represents the upper ball offset distance.

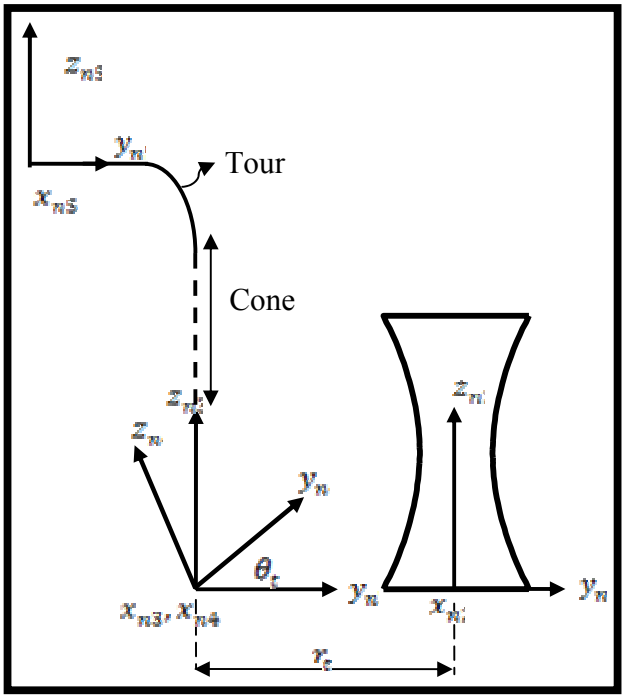

Figure (8) Transformation from S_{n2} to S_{n5}

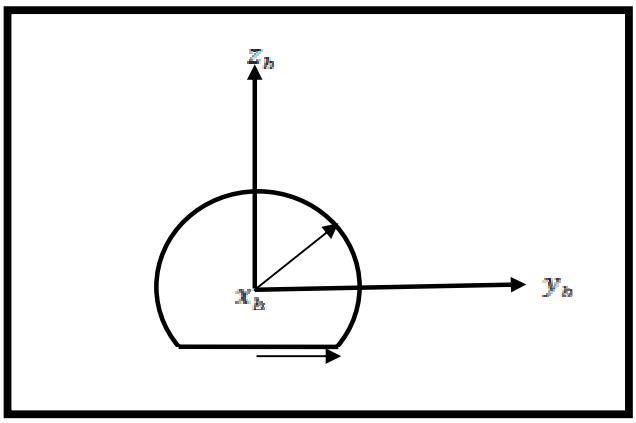

Figure (9), Upper Sphere Cross Section.

In Figure (10) the coordinate transformation from S_{b1} to S_{b2} are:

$$\left.\begin{aligned} x_{b2} &= x_{b1} \\ y_{b2} &= y_{b1}\, Cos(\theta_t) + z_{b1}\, sin(\theta_t) \\ z_{b2} &= z_{b1}\, cos(\theta_t) - y_{b1}\, sin(\theta_t) \end{aligned}\right\} \quad (18)$$

The last coordinate transformation is shown in Figure (11) and as follow:

$$\left.\begin{aligned} x_{b3} &= x_{b2} \\ y_{b3} &= y_{b2} - r_t\,(1 - Cos(\theta_t)) - r_{on}\, sin(\theta_1 + \theta_2)\, sin(\theta_t) \end{aligned}\right\} \quad (19)$$

$$z_{b3} = z_{b2} + l + r_t \sin(\theta_t) + r_{on} \sin(\theta_1 + \theta_2) \cos(\theta_t)$$

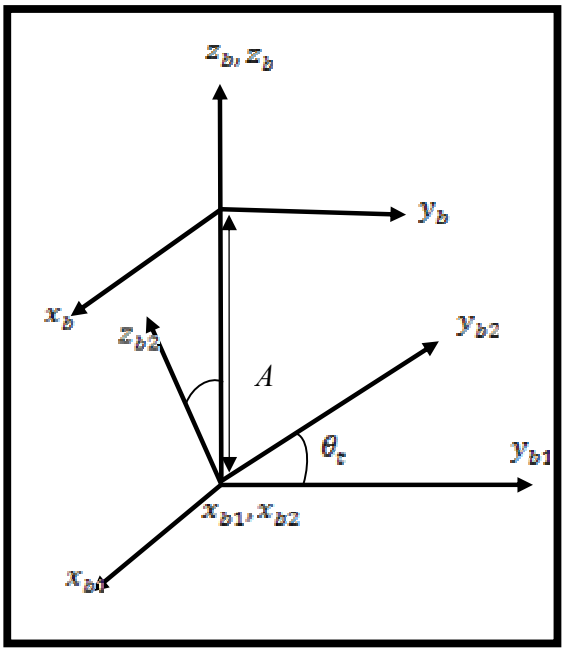

Figure (10), Transformation Coordinate System.

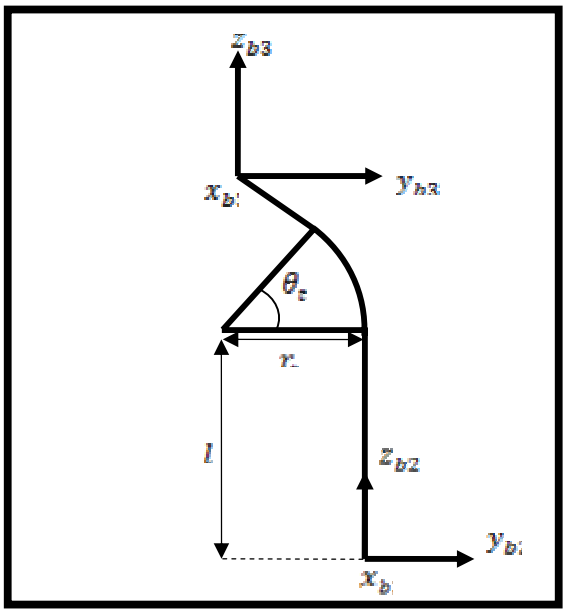

Figure (11),Transformation from S_{b2} to S_{b3}.

3. F.E. Stem Modeling:

Modeling steps of stem are:-

1- Build up the model .
2- Specify the material properties (module of elasticity and Poisson's ratio)
3- Specify the elements by using convergence test to choose the proper element type and number as following:

- Building up the stem models.
- Specifying the material properties as a structural, Titanium alloy, linear, elastic, isotropic with ν= 0.32, E= 110,000 N/mm^2 [Oguz Kayabasi and Fehmi Erzincanli, 2006].
- Specifying the applied load and boundary conditions (they are the same through the convergence test).
- Specifying the element type as solid and using the following element type successively (anasio 64, Tetrahedrol 10 node 187, 8 node 185, 20 solid 186, 20 solid 95, Brick 8 node 45 and 10 node 92) with changing the coarser to each element in order to investigate the right element number as well the element type. The result of the convergence test show that the best element type that can be employed to mesh the model is solid element 92 with 24403 elements and 36343 nodes as in Figure (12), and Figure (13) [Nassear Rasheid, 2009].

4- Apply load to the model using a concentrated load with contact algorithm the load at each hip joint is maximum.

The force was applied to concave surface of the whole of the acetabular.

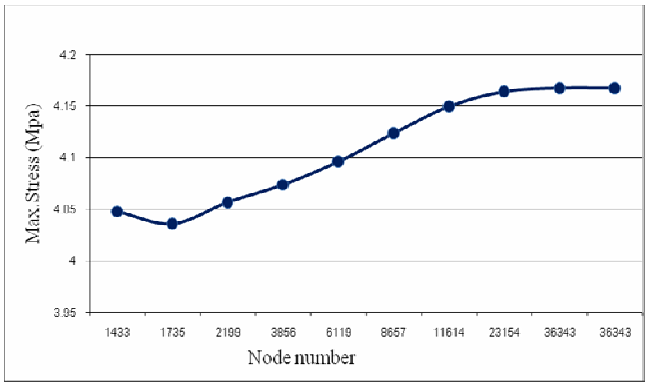

Figure (12), Convergence Test.

3.1 modeling of Contact Flement:

In most mechanical and structural engineering systems interactions occur between mechanical components or two parts of a single component when they contact with each other. Contact problems are highly nonlinear and required significant computer resources to solve [James F. Doyle, 2004].

Generally the contact problems can be put in two classes [R.B. Heywood, 1969]

1. Rigid- to- flexible bodies in contact problem: in this types of contact one or more of the contacting surfaces are treated as being rigid material, which has a much higher stiffness relative to deformable body it contacts. Many metals forming problems fall into this category. This type of contact problems is used for stem in mesh.
2. Flexible- to flexible bodies in contact: both contacting bodies are deformable. This type of contact problems is used for bolted joints, and interference fits.

3.2 Contact Element Capability:

Ansys finite element analysis (FEA) program offers a variety of elements designed to treat cases of changing mechanical contact between the parts of an assembly or between the different parts of different faces of a single part. These elements range from simple, limited idealizations to complex and sophisticated [Sandro Barone and Paola Forte, 2001]. In general the contact applications can be classified into three types [Oguz Kayabasi and Fehmi Erzincanli, 2006].

1. Point- to- point contact, where the exact location of contact should be known beforehand.
2. Point- to- surface contact, where the exact location of the area may not be known beforehand.
3. Surface- to- surface contact typically used to model surface- to – surface contact applications of rigid- to – flexible classification, Which is used in this work.

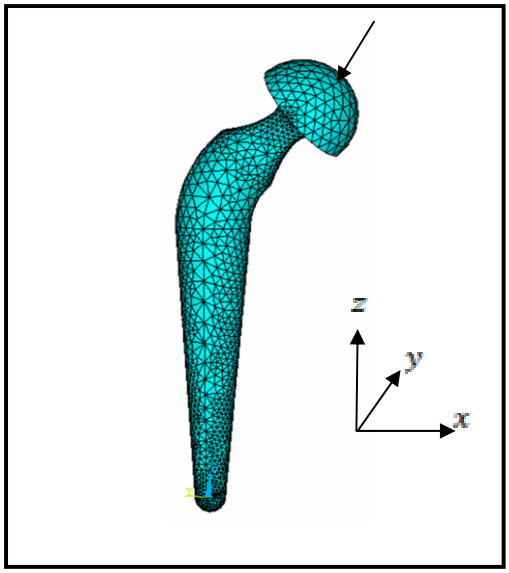

Figure (13), Stem Meshed with Solid Element 10 Nodes 92.

3.3. Material And Geometry Of Model:

The material used in this study is Titanium alloy (Ti6Al4V) with modulus of Elasticity (E) =110,000 N/$mm^2$and ν=0.32 .The properties of prosthesis design which are used in finite element method are the same properties of([Oguz Kayabasi and Fehmi Erzincanli, 2006]).

3.4. Loading Conditions:

For dynamic analysis, the maximum stumbling resultant force that applied on the surface of the implant bearing is 8.7 times the body weight (BW = 70 kg) applied at cup tip. This could be resolved into [H.F El'sheikh et al, 2003]: F_x = 2188.86N, F_y = −669.53N and F_z =−5472.1N

4. Fatigue Definition:

Fatigue is the failure of a material under fluctuating stresses each of which is believed to produce minute amounts of plastic strain[E.J.Hearn], failure is the sudden fracture after initiation and growth of a crack.

There are three factors affected on fatigue:

1. Crack length.
2. Cyclic stress.
3. Environmental conditions.

This factors affected on number of stress cycles before the final failure [Ayad Morad Alzuhairy, 2000].

5. Verification Test:-

The validity of the present work results must be checked by making a comparison with any previous work dealt with the same problem. The adopted work investigated the induced stresses in a special feature of Charnley stem by making neck cross section larger than the tour cross section (collar) under cyclic loading. The finite element model was meshed by solid 45 tetrahedron elements with total number of (10493). The applied load is used as a concentrated load with three components directed in (x, y, z) direction applied at the upper ball tip. Table (1) represents Verification of present work fatigue stresses with Ref.[Oguz Kayabasi and Fehmi Erzincanli, 2006].

Table (1) Verification of present work fatigue stresses with Ref.[Oguz Kayabasi and Fehmi Erzincanli, 2006].

Max. Equivalent Stress (MPa)	Max.Equivalent Stress(MPa),present work	Percentage Error (%)
207.447	204.44	1.4495
184.395	175.98	4.564
161.348	152.6	5.422
138.298	131.68	4.785
115.249	108.29	6.038
92.199	85.314	7.467
69.149	63.614	8.004
46.099	44.904	2.592
23.050	21.607	8.008

6. Results and Discussions:

The mechanical failure of femoral stem of total hip replacement prosthesis occurs not infrequently, probably as a result of cyclic stress above endurance limit of implant material. A good implant design should satisfy maximum or an infinite fatigue life endurance fatigue effects on stem. This can be insured by physical testing or a fatigue analysis.

The effects of surgical mechanics of implantation, prosthetic design and the prosthetic material appear to be inter related. In present study the effects of a series of variables on stress in the femoral stem and fatigue life of the prosthesis are analyzed, the variables include:-

1. Angle of neck.
2. Ball radius.
3. Main tour Radius.

4. Neck ratio.
5. Outer tour radius.
6. Radius of neck.

Figure (14) shows contour distribution of Von mises stress values due to change of effective design parameter (neck angle). While of figure (15) show contour of minimum safety factor values which calculated according to Soderberg theory due to change of the same parameters.

The variation of equivalent (Von mises) stresses under periodic loads are shown in figures (16) to (27).

From the results it is clear that the most dominant design parameter is (outer tour radius (r_o)) which has found to reduce the Von mises stress by 226 MPa because the decreasing for the moment inertia see figure (22) and increase the safety factor by 1.5 as shown in figure (23).

The second effective design parameter is the neck angle which has a direct relationship with the Von mises stresses, it is clear that the increasing of the neck angle increases the arm of the bending moment (increasing Von mises stress by 100 MPa) as shown in figure (16) and an inverse one with safety factor (decreasing the safety factor by 1.5) as shown in figure (17).

The third effective design parameter is the radius of neck which has been found to has an inverse correlation with the max. Von mises stress in the range of (10) mm to (16) mm (decreasing the Von mises by100 MPa), the cause of that is the increasing of the moment of the inertia at the neck section, see figure (24) and a direct one with safety factor increasing the safety factor by 6) as in figure (25).

The fourth effective design parameter is the ball radius which found to has a direct relationship with the Von mises stresses in the range of (15-25) mm (increasing the Von mises stresses by 45 MPa), this is due to that increasing of the arm of the pressure center so that the bending moment increases, see figure (18) and an inverse one with safety factor in

The same range (decreasing the safety factor by 0.8) see figure (19).

The fifth effective design parameter is the neck ratio which has found to has an inverse relationship with the max. Von mises stress in the range of (0.5) to (0.8) mm (decreasing the Von mises by 30 MPa) as shown in figure (26) and has a direct one with safety factor in the same range (increasing the safety factor by 0.75) as shown in figure (27).

The sixth effective design parameter is the tour main radius (r_t) which has insignificant effect on the max.Von mises stresses and safety factor because the arm of the bending moment increasing with the increasing of mean tour radius as presented in figures (20),(21).

7. Conclusions:

1. It was found that the outer tour radius play a key role in decreasing the fatigue stresses by (175) MPa in the range of (10 to 15) mm, radius of the neck and neck raio play the same role but with a lower effect.
2. The values of the neck angle and ball radius must be as lower as possible because they have a negative effect on the max. fatigue stresses.
3. Despite of the major positive role of the outer tour radius there is a minor negative role and that is the moving of the max. Fatigue stress zone to the weakest stem section (neck) from the tour section.
4. The radius of neck has the dominate role and increasing the safety factor from (1.2 to 7.2), while the neck ratio and outer tour radius have a lower direct effect. The increasing of the neck angle and ball radius decreases the safety factor.

8. References

Ayad Morad Alzuhairy, (Study of fatigue properties of acicular ductile iron compared with steel(42 CrMo4)), M.Sc.thesis, University of technology, 2000.

E. J. Hearn, (Mechanics of materials), Book, International series on material science and technology, VOL. 19, 1977.

Fumihiro Yoshiminea, Ko Ginbayashi(A mathematical formula to calculate the theoretical range of motion for total hip replacement), Journal of Biomechanics, 35 (2002) 989–993,www.elsevier.com/locate/jbiomech

H.F El'sheikh, B.J MacDonald, M.S.J. Hashmi, (Finite element simulation of the hip joint during stumbling: a comparison between static and dynamic loading), Journal of materials processing technology143–144 (2003) 249–255.

James F. Doyle, (Modern experimental stress analysis), Book, Purdue University, Lafayette, USA, 2004.

Kassim A Abdullah, (Stress and stability analysis of the neck – stem interface of the modular hip prosthesis), Ph.D. thesis , Queen's university –Mechanical engineering ,Canada 1997.

Nassear Rasheid Hmoad, (Simulation of meshing and contact with stress analysis of hypoid gear drive), M.Sc. thesis, Baghdad university ,library of Mechanical engineering , 2009.

Niel Pieterse, (Development of a dynamic hip joint simulation model),M.Sc. thesis, University of Pretoria, 2006

Oguz Kayabasi and Fehmi Erzincanli,(Finite element modeling and analysis of a new cemented hip prosthesis), ELSEVIER, Advances in Engineering Software 37 (2006) 477–483.

R.B. Heywood, (Photoelasticity for designers), Vol. 2, 1969.

Sandro Barone and Paola Forte, (CAD / FEM procedures for stress analysis in unconventional gear applications), International Journal of computer applications in technology), Vol. 15, No. 1, 2001, pp.305-389.

9. Nomenclatures

English Symbols

Symbol	Description	Unit
A	Upper ball distance offset	mm
E	Modulus of elasticity	N/ mm^2
F	Force	N
n_r	Neck ratio=the position of the neck weakest section to neck length	
N	safety factor	
o_c	Tour circle center	
o_t	Main tour circle center	
r_b	Ball radius	mm
r_i	The bottom sphere radius, the bottom cone radius	mm
r_n	Neck radius	
r_o	The upper cone radius, the outer cone radius	mm
r_{on}	The outer radius of neck	
r_t	Main tour radius	
R_s	Stress ratio	
$S_n(x_n, y_n, z_n)$	The coordinate system of Neck	
x, y, z	Cartesian coordinate	

10. Greek symbols

Symbol	Description	Unit
θ_t	The tour angle or Neck angle	degree
θ	Angle between project (r_i) on (x-y) plane and (x) axis in spherical coordinate system.	degree
ν	Poisson's ratio	-
σ_{max}	Maximum stress	MPa
σ_{min}	Minimum stress	MPa
ϕ	Angle between (r_i) and project (r_i) on (x-y) plane	Degree

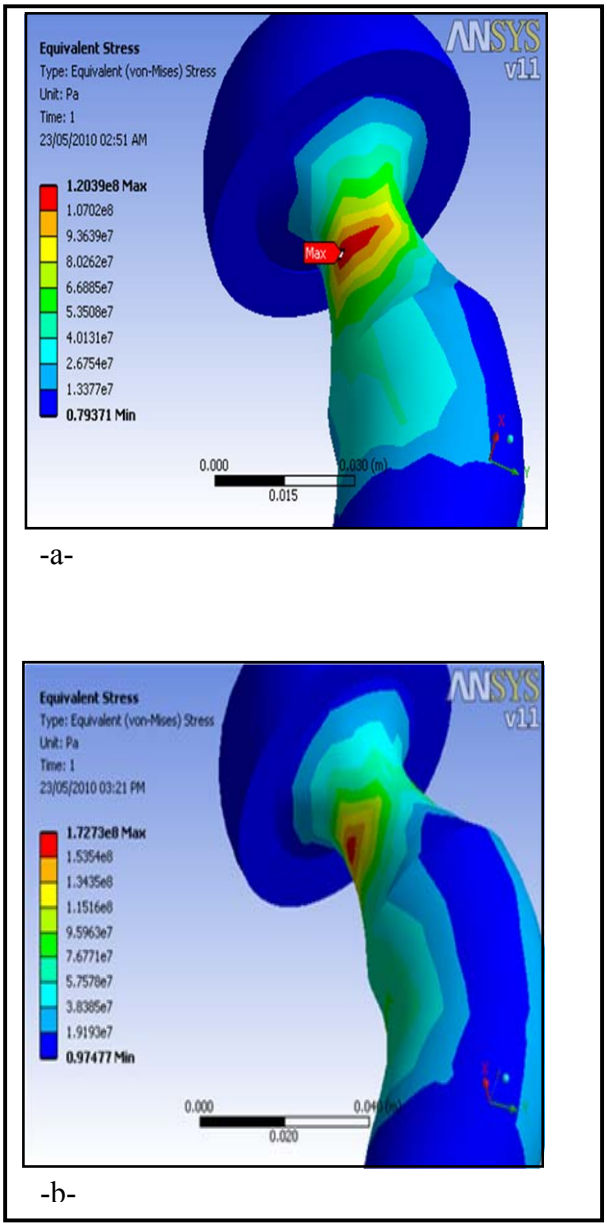

Figure (14), Von mises Stress with Changing Neck Angle. (a)-θ_c=35°, (b)- θ_c=55°

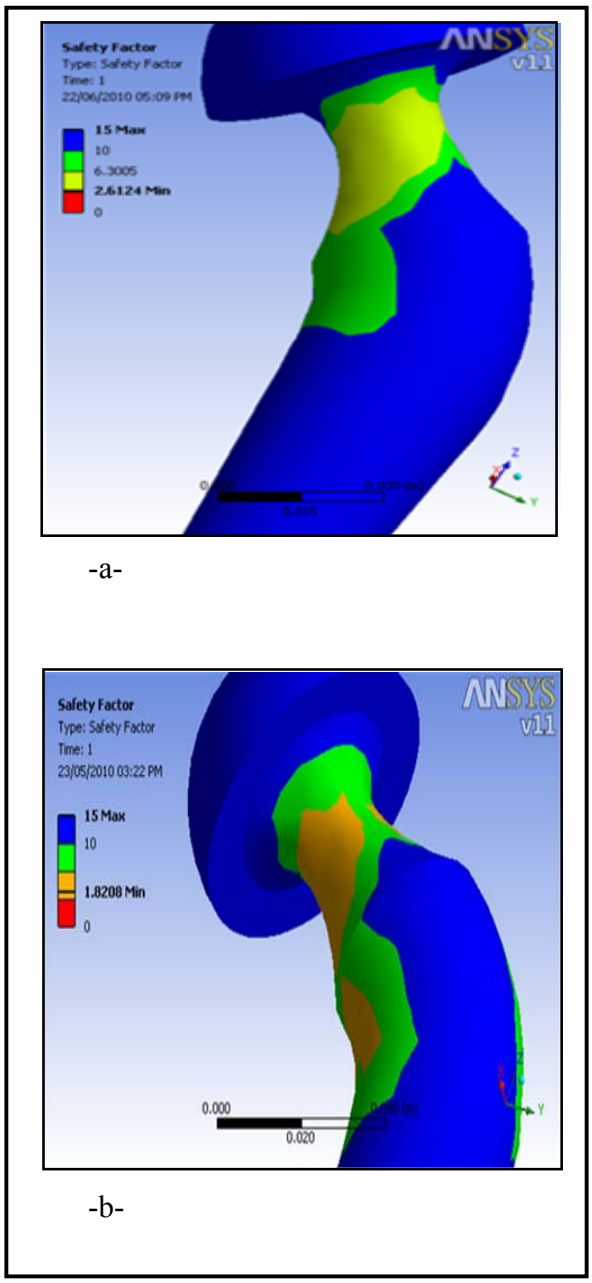

Figure (15), Safety Factor with Changing Neck angle. (a)-θ_c=35°, (b)- θ_c=55°

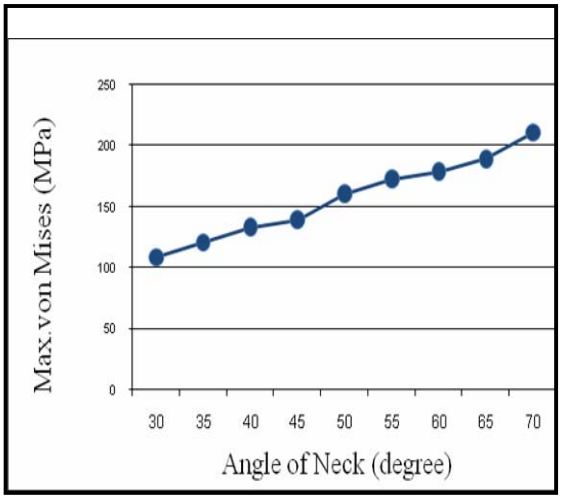

Figure (16), Variation of Max.Von mises Stress with Angle of Neck.

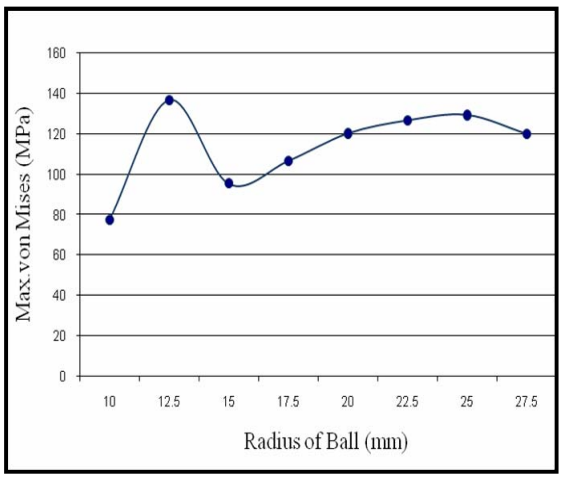

Figure (18), Variation of Max.Von mises Stress with Ball Radius.

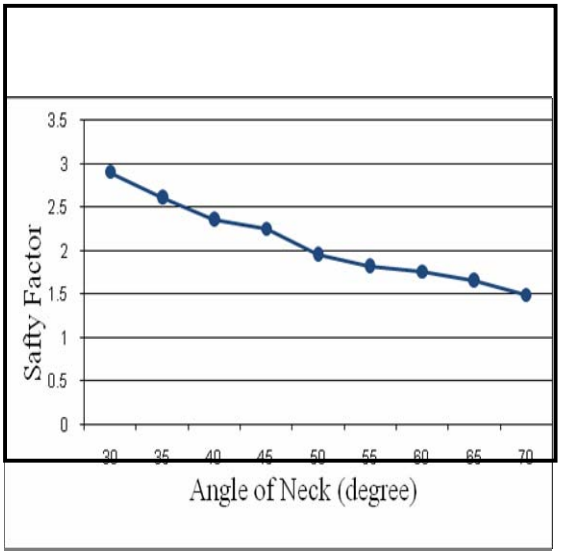

Figure (17), Variation of Min. Safety Factor with Angle of Neck.

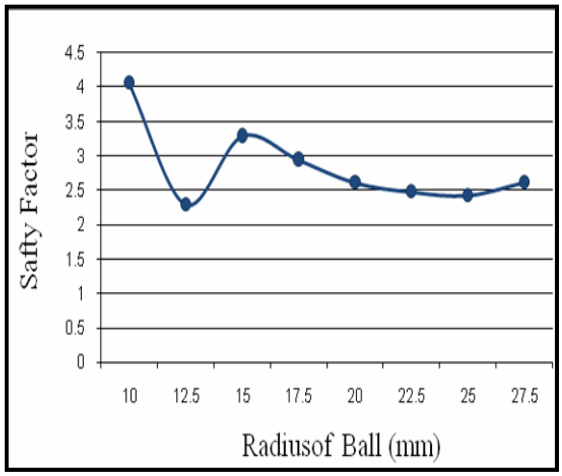

Figure (19), Variation of Min. Safety Factor with Ball

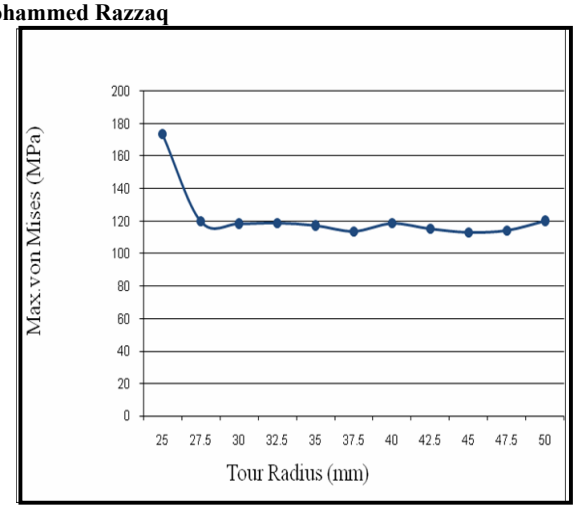

Figure (20), Variation of Max.Von mises Stress with Main Tour Radius.

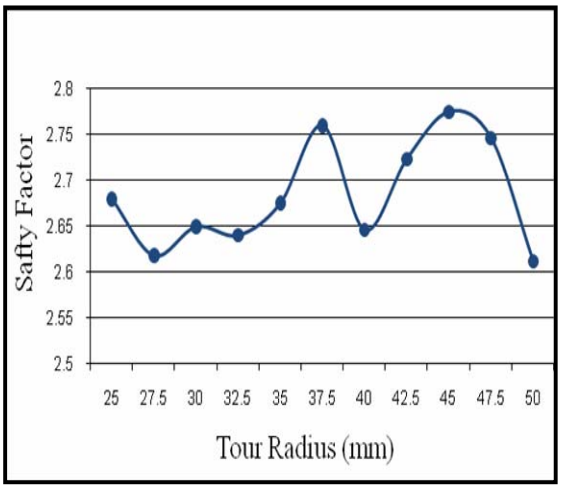

Figure(21), Variation of Min. Safety Factor with Main Tour Radius.

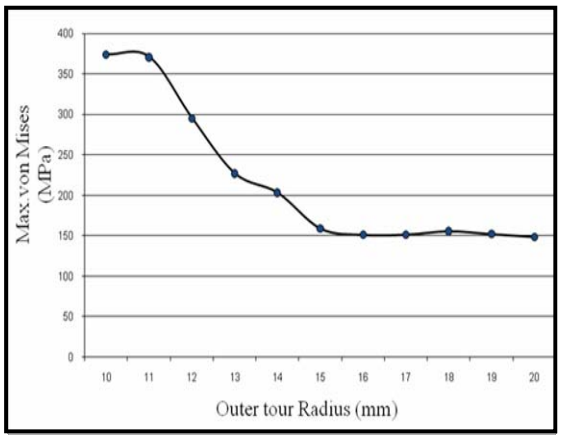

Figure (22), Variation of Max.Von mises Stress with Outer Radius of Tour.

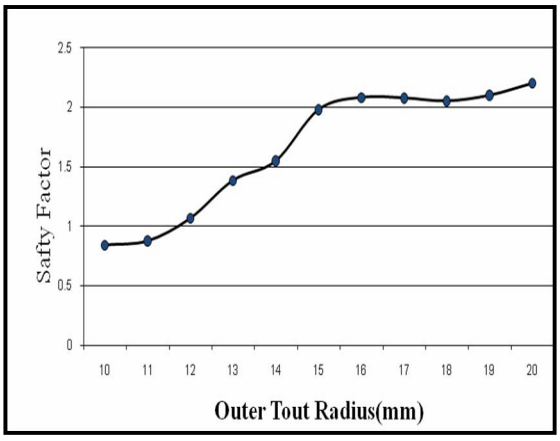

Figure(23), Variation of Min. Safety Factor with Outer Radius of Tour.

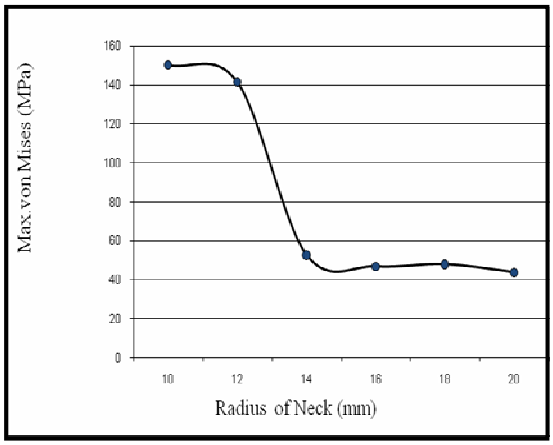

Figure(24), Variation of Max.Von mises Stress with Neck Radius.

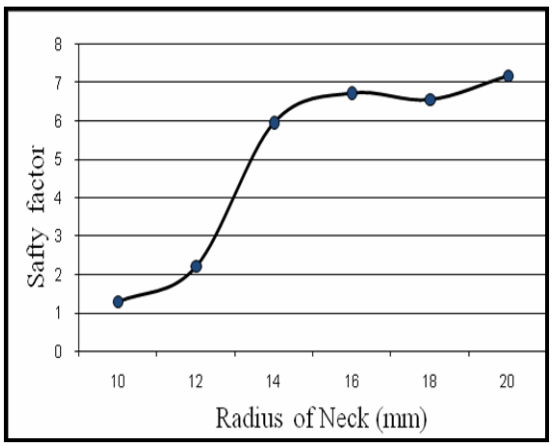

Figure(25), Variation of Min. Safety Factor with Neck Radius .

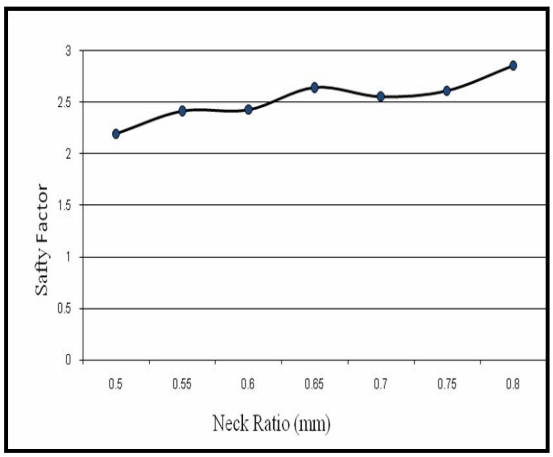

Figure (27), Variation of Min. Safety Factor with Neck Ratio.

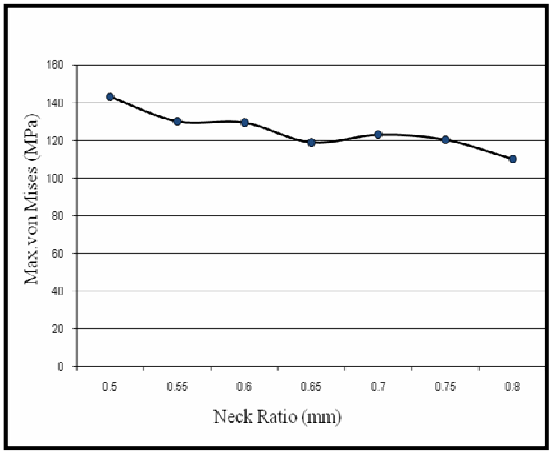

Figure (26), Variation of Max. Von mises Stress with Neck Ratio.